USE OF COLLOIDAL CRYSTAL SELF-ASSEMBLY METHODS FOR THE PRODUCTION AND STUDY OF POLYMETHYL METHACRYLATE COLLOIDAL CRYSTALS

Supported by tetfund

E.C. Ajiduku and E.A. Kamba*
Department of Chemical Sciences, Federal University, Wukari. Taraba State. Nigeria
*Corresponding author**:** eacambah@gmail.com

Abstract

Two different self-assembly techniques were used to successfully fabricate polymethyl methacrylate (PMMA) colloidal crystals: vertical deposition by evaporation approach as well as a modified floating (i.e. air-water interface) approach. Also, temperature dependent study using the vertical deposition was conducted. PMMA colloidal crystals with monolayer were produced via the floating approach. When deposited multiple times, 3D double-layered as well as triple-layered colloidal crystals were successfully fabricated. Furthermore, an investigation of the photonic properties of the PMMA colloidal crystals was carried out. The results show that the crystals were opalescent when illuminated and also had a typical photonic stop band which lies in the visible region of the spectrum.

Keywords: Colloidal, polymethyl methacrylate, self-assembly, photovoltaics

Introduction

It has been reported that upon PMMA colloidal spheres formation through the SFEP process, they can self-assemble into colloidal crystals (Hussain et al., 2010). These highly ordered close-packed structures can be used as templates to synthesize inverse opals as well as photonic crystals which can applied in a variety of areas including photovoltaics (Waterhouse and Waterland, 2007a).

By changing several parameters in the experimental conditions, such as type of the substrate, concentration of the colloidal spheres and rate of solvent evaporation can result in achieving a controllable thickness of the colloidal crystals (Levesque and Seeberger, 2011). However, achieving total control of the colloidal crystal thickness remains a challenge. Considering that monolayer colloidal crystals can be produced by the floating technique, it is theorized that by repeating the technique on the same deposited substrate multiple layers may be created using this technique. The success of such an approach it will be a powerful, facile technique for the production of 3D colloidal crystals having controlled thickness.

Due to their periodic structures constructed from alternating regions of refractive indices, colloidal crystals can be seen as photonic crystals, hence, the successful fabrication of colloidal crystals can result in a photonic stop band in the visible region (Gilmore and Seeberger, 2014). It is possible to tune the colours in colloidal crystals that act as photonic crystals by applying external physical or chemical stimuli (Bedi et al., 2013). It is also possible to alter the photonic stop band characteristics by varying the refractive index contrast. The photonic stop band can be used to calculate the diameter of the original PMMA colloidal sphere by applying a modified form of the Bragg's equation of diffraction (Levesque and Seeberger, 2011; Gilmore and Seeberger, 2014). The photonic properties of PMMA colloidal crystals fabricated by the floating technique have been investigated in this work.

Experimental Procedures

Vertical Deposition approach for Fabrication of PMMA Colloidal Crystal

For colloidal crystal fabrication experiments a previously synthesised PMMA sphere solution via SFEP process using 6 ml of MMA monomer (with average sphere diameter of 414 nm) was used. After centrifuging, the top water was decanted and the white spheres (residues) were dried in an oven at 40°C for 6 hours. The drying was followed by preparation of a suspension of PMMA spheres in water (1.5 wt %). 25 ml of the PMMA suspension was then placed in a 50 ml glass beaker. Meanwhile, a microscope glass slide was etched for 1 hour in sodium hydroxide solution (30 wt%) in order to increase its hydrophilicity, for enhanced attachment of the PMMA sphere (Keulemans *et al.*, 2016). This was followed by thoroughly washing the glass slide with DI water several times and then suspending it in the beaker. The beaker and the suspended slide was then placed in an oven at fixed temperature for 48 hours. This resulted in evaporation of the water in the beaker leaving behind a white film of the closed-packed PMMA colloidal crystal on the glass slide. Finally, effect of temperature on the colloidal crystal quality was evaluated using five different oven temperatures of 51°C, 62°C, 72°C, 84°C and 93°C.

Floating Approach for the Fabrication of PMMA Colloidal Crystal

3 ml of PMMA spheres solution previously produced using SFEP process (average sphere diameter of 383 nm) was mixed with 3 ml ethanol in a small vial in a 1:1 ratio by volume. A 2 cm^2 piece microscope glass slide was then cleaned by ultra-sonication in acetone followed by in DI water for 10 minutes. Then, placing the glass in the center of a Petri dish, DI water was added into the Petri dish, until it covered the sides of the glass specimen without covering its surface. A drop of the solution of PMMA-ethanol was placed on the centre of the glass using a pipette. From one side of the petri dish, more DI water was carefully added until the water level rose to cover the surface of the glass and just touched the PMMA-ethanol solution contact line without submerging PMMA-ethanol. Due to the differences in surface energy between the solution and the water in the Petri dish, the PMMA solution rose to the top of the water

surface (Gupta and Tripathi, 2011; Tahir and Amin, 2013). After a few seconds, an iridescent monolayer island of PMMA colloidal crystal was formed on the water surface. In order to facilitate the next step of picking the colloid crystal on to a substrate, more water was carefully added to the Petri dish to raise the water level (Xiong et al., 2012). To fabricate a double layer colloidal crystal, the above procedure was repeated on the same substrate once the deposited monolayer colloidal crystal was fully dry. The procedure was repeated until the desired number of layers of PMMA colloidal crystal was obtained.

Results and Discussion

Temperature Dependent Vertical Deposition Technique

The five samples produced at the different temperatures via the vertical deposition technique for 3D multiple-layered colloidal crystal fabrication showed self-assembled PMMA spheres with high quality colloidal crystal. No obvious systematic difference in thickness within the experimental temperature range was observed. Figure 1 shows the Scanning Electron Microscope (SEM) images for the PMMA colloidal crystal produced at (a) 51°C, (b) 72°C and (c) 84°C. All the SEM images in Figure 1 show highly ordered close-packed structures. The PMMA structures tend to be FCC with their (111) planes parallel to the underlying substrate. This configuration is thermodynamically favoured (Bou-Hamdan and Seeberger, 2012; Inde *et al*., 2016), however, Lévesque and Seeberger, (2013) countered an assumption that the preferred FCC crystal structure embedded in self-assembly processes is solely driven by thermodynamic equilibrium. Instead, they suggest it is one of the dynamic self-assemblies in which viscous drag due to the fluid flow within the sphere pores form such a structure. The confinement space between the air pores of touching spheres in 3D PMMA colloidal crystals formed by the ABCABC stacking of the FCC structure can be determined mathematically (Yan et al., 2016). Assuming r is the radius of PMMA spheres, then the confinement space within the tetrahedral and octahedral cavities (pores) can be estimated by spheres of radius 0.225r and 0.414r respectively. The largest particle, which has a spherical shape that can pass freely through cavities has a radius of 0.156r.

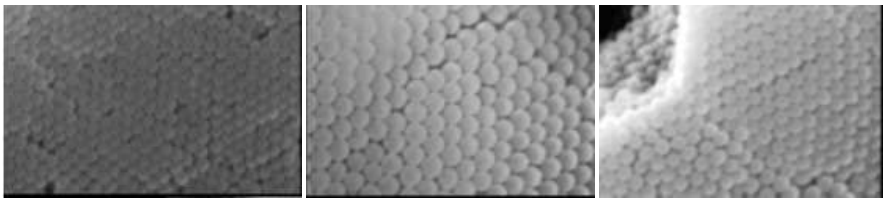

Figure: 1 SEM images depicting 3D multilayered PMMA colloidal crystals fabricated using vertical deposition technique at 51°C, 72°C and 84°C from left to right respectively.

A 2-3% reduction in diameter during colloidal crystal formation of samples was observed. The reduction may be attributed to condensation and loss of water in each sphere during drying or the deposition process as the raised temperature was raised. Interestingly, sphere diameter shrinkage is approximately the same for all of the samples, indicating that sphere size is independent of temperature at these medium-range temperatures. Another important phenomenon observable with increase in temperature is the formation of necking (i.e. connection between the spheres), which becomes more obvious as temperature increases. The necking between the PMMA spheres for the self-assembled sample at 93°C can be seen in the SEM image in Figure 2.

Figure: 2 SEM image depicting necking between self-assembled PMMA spheres in a colloidal crystal at 93°C.

This phenomenon occurs when capillary forces pull the spheres together during the self-assembly process; it can also lead to the increase in the distance between the spheres (Figure 2) (Gupta and Tripathi, 2011). Necking phenomenon can be important as it increases the mechanical strength of colloidal crystals, and can be beneficial for processes such as fabrication of inverse opal.

Another observation made in the samples is the change in the quality of the colloidal crystals at different areas of the film. This phenomenon was observed in Figure 3, which shows an SEM image taken at just below the original meniscus contact line (i.e. air-water-substrate) of the vertically deposited self-assembled sample at 93°C.

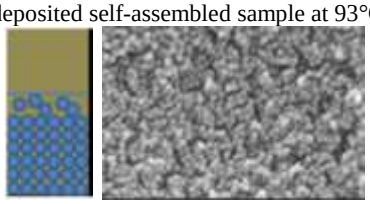

Figure 3: Schematic representation and SEM image showing PMMA self-assembly taken just below the original meniscus contact line.

It can be seen from schematic diagram and the SEM image in Figure 3, that there is a portion of spheres that is loosely floating around, hence, the spheres are not completely self-assembled into an ordered colloidal crystal at this region. This phenomenon can be due to the low concentration of the spheres at the area just below the meniscus contact line. The quality of the self-assembly is further enhanced down the film as shown in Figure 3. This indicates that a concentration gradient in this technique (vertical deposition) self-assembly technique, exists and can be

attributed to the gradual evaporation of water inside the beaker, which leads to the increase in concentration of the spheres in the solution. As such, more spheres are available at the bottom of the beaker leading to better self-assembly at the bottom region of the glass substrate, positioned vertically in the beaker. Moreover, due to this concentration gradient, the film at the bottom of the glass substrate tends to be thicker than that at the top. If the film becomes excessively thick, it can consequently result in shearing, cracking and eventually peeling off the glass substrate, leaving some bare areas at the bottom of the substrate.

Aside concentration gradient, other factors may also be responsible for the formation of these macroscopic cracks. The gravitational forces, for instance, can lead to the water inside the sphere solution to move downwards, resulting in the formation of paths among the spheres as cracks (Bou-Hamdan et al., 2011; Mei, Pougin and Strunk, 2013).

Floating Deposition Approach

Figure 4 shows the SEM images of the monolayer colloidal crystal film removed from the water surface by a glass substrate.

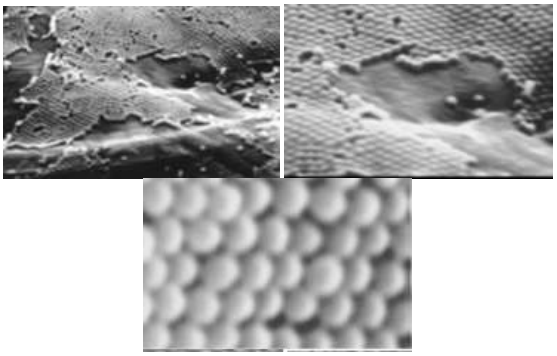

Figure 4: 10µm, 5µm and 1µm magnification from left to right respectively of SEM images of monolayer PMMA colloidal crystal fabricated via the floating approach.

The average size of the PMMA spheres after self-assembly remains fairly constant (c. 383 nm). Large areas of monolayer 2D colloidal crystals are formed without any cracks (Figure 4). A low level of defects in the form of separate spheres on top of the monolayer can be detected, which may arise due to spheres that are mixed up with the water in the Petri dish instead of staying afloat.

In the floating approach, one of important steps is the deposition of the colloidal spheres onto the surface of the liquid. This is so because they can easily sink and disperse into the bulk of the liquid. If water is used as the liquid, equal volume of ethanol will be required to be added to the colloidal sphere solution prior to depositing onto the water surface. The ethanol added acts as a spreading agent since water-ethanol mixture has lower density than pure water (0.911 compare to 1 g/cm3), thus when used, the floating of the PMMA sphere is enhanced (Fujishima, Zhang and Tryk, 2008; Khan, Adil and Al-Mayouf, 2015). Furthermore, addition of ethanol improves the hydrophobic nature of the solvent, which is also beneficial to improve the dispersion of the PMMA spheres.

As observed in Figure 5, fabrication of uniform 3D multi-layered PMMA colloidal crystal films with large coverage areas can be using the floating approach is possible. One of the advantages of this technique over others, such as vertical deposition, is its display of versatility. This include: the ability of the colloidal crystals can stack over each other irrespective of the sizes, morphologies or even composition owing to the layer-by-layer nature of the floating depositions on the substrate.

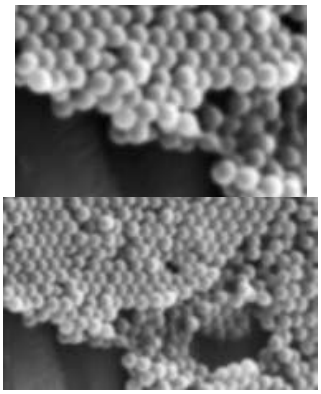

Figure 5: SEM images of 3D PMMA colloidal crystals formation achieved by repeating the floating deposition twice to produce double-layers (left) and thrice to produce triple-layers (right)

Nevertheless, some defects can appear on the surface of multilayer films, which may be due to spheres mixing in the water during substrate removal. Detectable small cracks on the surface when more layers are added to the colloidal crystal film can be attributed to the electrostatic attractions between the substrate and the colloidal spheres as the spheres are lifted up from the water surface (Waterhouse and Waterland, 2007).

Photonic Properties of PMMA Colloidal Crystals

Figure 6 shows the images of typical monolayer PMMA colloidal crystal film that was deposited on a microscope glass slide substrate through the modified floating technique with (left) and without (right) illumination. The range of colours detected during irradiation are due to diffraction of visible light by the colloidal crystal, which possesses a periodic array of low and high refractive index areas of air and PMMA spheres (Hurevich et al., 2014).

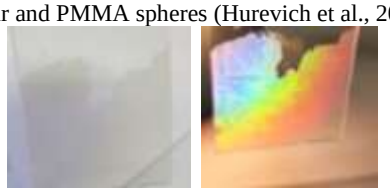

Figure 6: Monolayer PMMA colloidal crystal film with (left) and without (right) visible light illumination.

The colour change phenomenon observed in Figure 6 does not depend on electronic processes observed in most other colour displaying materials, whose colours are due to the absorption of visible light, which leads to electronic transitions that absorb or emit specific bands of light (Kim, 2008). PMMA colloidal crystal has ability to "filter" light, a peculiar property, which makes it act as a photonic crystal. In general, when white light is irradiated on such

structures, some wavelengths are prohibited from passing through the colloidal crystal and so are reflected instead, while the remaining wavelengths, which are unaffected by the colloidal crystal are allowed to pass through.
Normal incidence reflectance spectrum of the monolayer PMMA colloidal was obtained using a UV-Vis reflectance spectrometer and λ_{max} extracted as shown in Figure 7.

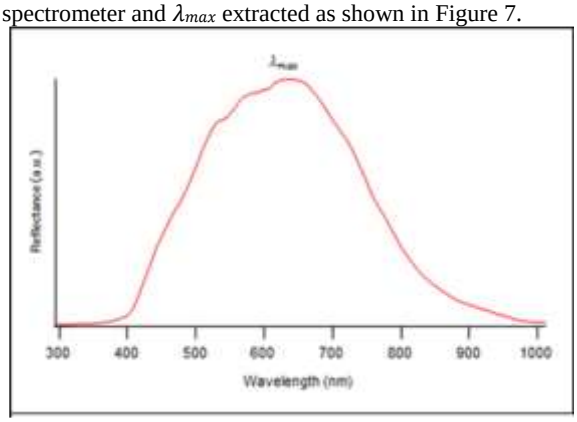

Figure 7: UV-Vis reflectance spectrum of a monolayer PMMA colloidal crystal.

From Figure 7, the reflectance maxima (λ_{max}) is positioned at 627 nm, while the PMMA Sphere diameter (D) was calculated to be 281 nm.
This value however, is 27% less than the original average sphere diameter as determined by the SEM, which is 383 nm. The discrepancy may be due to crystal defects and size distribution of the PMMA spheres. Such defects of the spheres may also cause interference with the diffraction of light (Balaji et al., 2011; Wang and Jing, 2014; Yan et al., 2016). Although the sphere diameter is not in good agreement with the SEM analyses, the photonic crystal properties of the PMMA colloidal crystal is seen in the existence of the reflectance maxima (λ_{max}) (Waterhouse and Waterland, 2007).

4.0 Conclusion

The two techniques employed for fabrication of PMMA colloidal crystals in this work both showed high quality ordered self-assembled PMMA spheres. The modified floating technique can be considered as a powerful yet simple technique for colloidal crystal fabrication. Its simplicity as well as output of large areas of opalescent monolayer or multilayer photonic colloidal crystals within a short timeframe makes it an attractive technique. In addition, its multiple deposition abilities make it easy to control the thickness of the colloidal crystals. The PMMA colloidal crystals also demonstrated photonic crystal properties making them good candidates for several applications as in templating techniques for production of inverse opals as well as opalescent materials several other applications, including sensors, decoration, information storage, displays, and camouflage (Waterhouse and Waterland, 2007; Bedi et al., 2013).

Recommendation

The monolayer colloidal crystals produced can be used in templating procedures for applications in photoelectrochemical water splitting as well as solar cell experiments. Conductive substrates such as titanium metal and FTO glass are of great interest for PMMA colloidal crystal deposition and should be exploited. The colloidal crystal film can cover large surface of titanium plate, which makes it a good candidate for templating as well as photovoltaic processes. The modified floating self-assembly approach is considered as a convenient technique by which large areas of high quality, monolayer PMMA colloidal crystals can be produced, and can be converted further to 3D multilayers with a well-controlled thickness.

References

Balaji, S. et al. (2011) 'Porous orthorhombic tungsten oxide thin films: synthesis, characterization, and application in electrochromic and photochromic devices', Journal of Materials Chemistry, 21(11), p. 3940. doi: 10.1039/c0jm03773g.

Bedi, J. S. et al. (2013) 'Electrospinning of poly(methyl methacrylate) nanofibers in a pump-free process', Journal of Polymer Engineering, 33(5), pp. 453–461. doi: 10.1515/polyeng-2012-0096.

Bou-Hamdan, F. R. et al. (2011) 'Continuous flow photolysis of aryl azides: Preparation of 3H-azepinones', Beilstein Journal of Organic Chemistry, 7(Scheme 1), pp. 1124–1129. doi: 10.3762/bjoc.7.129.

Bou-Hamdan, F. R. and Seeberger, P. H. (2012) 'Visible-light-mediated photochemistry: accelerating Ru(bpy)32+-catalyzed reactions in continuous flow', Chemical Science, 3(5), p. 1612. doi: 10.1039/c2sc01016j.

Fujishima, A., Zhang, X. and Tryk, D. A. (2008) 'TiO2 photocatalysis and related surface phenomena', Surface Science Reports. doi: 10.1016/j.surfrep.2008.10.001.

Gilmore, K. and Seeberger, P. H. (2014) 'Continuous flow photochemistry', Chemical Record, 14(3), pp. 410–418. doi: 10.1002/tcr.201402035.

Gupta, S. M. and Tripathi, M. (2011) 'A review of TiO2 nanoparticles', Chinese Science Bulletin, 56(16), pp. 1639–1657. doi: 10.1007/s11434-011-4476-1.

Hayward, V. et al. (2006) 'References and Notes 1.', 445(June), pp. 1504–1508. doi: 10.1126/science.1231143.

Hurevich, M. et al. (2014) 'Continuous photochemical cleavage of linkers for solid-phase synthesis', Organic Letters, 16(6), pp. 1794–1797. doi: 10.1021/ol500530q.

Hussain, M. et al. (2010) 'Synthesis, characterization, and photocatalytic application of novel TiO2 nanoparticles', Chemical Engineering Journal, 157(1), pp. 45–51. doi: 10.1016/j.cej.2009.10.043.

Inde, R. et al. (2016) 'Ti(<scp>iv</scp>) nanoclusters as a promoter on semiconductor photocatalysts for the oxidation of organic compounds', J. Mater. Chem. A, 4(5), pp. 1784–1791. doi: 10.1039/C5TA08340K.

Keulemans, M. et al. (2016) 'Activity versus selectivity in photocatalysis: Morphological or electronic properties

tipping the scale', Journal of Catalysis. Elsevier Inc., 344(December), pp. 221–228. doi: 10.1016/j.jcat.2016.09.033.

Khan, M. M., Adil, S. F. and Al-Mayouf, A. (2015) 'Metal oxides as photocatalysts', Journal of Saudi Chemical Society, pp. 462–464. doi: 10.1016/j.jscs.2015.04.003.

Kim, H. J. (2008) 'The Transition from Paper to Electronic Journals', http://dx.doi.org/10.1300/J123v41n01_04. Taylor & Francis Group , 41(1), pp. 31–64. doi: 10.1300/J123V41N01_04.

Kopetzki, D., Lévesque, F. and Seeberger, P. H. (2013) 'A continuous-flow process for the synthesis of artemisinin', Chemistry - A European Journal, 19(17), pp. 5450–5456. doi: 10.1002/chem.201204558.

Levesque, F. and Seeberger, P. H. (2011) 'Highly efficient continuous flow reactions using singlet oxygen as a "Green" reagent', Organic Letters, 13(19), pp. 5008–5011. doi: 10.1021/ol2017643.

Mei, B., Pougin, A. and Strunk, J. (2013) 'Influence of photodeposited gold nanoparticles on the photocatalytic activity of titanate species in the reduction of CO2 to hydrocarbons', Journal of Catalysis. Elsevier Inc., 306, pp. 184–189. doi: 10.1016/j.jcat.2013.06.027.

Tahir, M. and Amin, N. S. (2013) 'Advances in visible light responsive titanium oxide-based photocatalysts for CO2 conversion to hydrocarbon fuels', Energy Conversion and Management. Elsevier Ltd, 76, pp. 194–214. doi: 10.1016/j.enconman.2013.07.046.

Wang, A. and Jing, H. (2014) 'Tunable catalytic activities and selectivities of metal ion doped TiO 2 nanoparticles – oxidation of organic compounds', Dalton Trans., 43(3), pp. 1011–1018. doi: 10.1039/C3DT51987B.

Waterhouse, G. I. N. and Waterland, M. R. (2007a) 'Opal and inverse opal photonic crystals: Fabrication and characterization', Polyhedron. Pergamon, 26(2), pp. 356–368. doi: 10.1016/j.poly.2006.06.024.

Waterhouse, G. I. N. and Waterland, M. R. (2007b) 'Opal and inverse opal photonic crystals: Fabrication and characterization', Polyhedron. Pergamon, 26(2), pp. 356–368. doi: 10.1016/J.POLY.2006.06.024.

Xiong, L. Bin et al. (2012) 'Ti 3+ in the surface of titanium dioxide: Generation, properties and photocatalytic application', Journal of Nanomaterials, 2012. doi: 10.1155/2012/831524.

Yan, M. et al. (2016) 'The fabrication of a novel Ag $_3$ VO $_4$ /WO $_3$ heterojunction with enhanced visible light efficiency in the photocatalytic degradation of TC', Phys. Chem. Chem. Phys. Royal Society of Chemistry, 18(4), pp. 3308–3315. doi: 10.1039/C5CP05599G.